

Effect of magnetic field annealing on soft magnetic properties of $\text{Co}_{71}\text{Fe}_2\text{Si}_{14-x}\text{B}_{9+x}\text{Mn}_4$ amorphous alloys with low permeability

Xingdu Fan, Meng Li, Tao Zhang, Chenchen Yuan, and Baolong Shen

Citation: *AIP Advances* **8**, 056105 (2018); doi: 10.1063/1.5006989

View online: <https://doi.org/10.1063/1.5006989>

View Table of Contents: <http://aip.scitation.org/toc/adv/8/5>

Published by the [American Institute of Physics](#)

Articles you may be interested in

[Structure and soft magnetic properties of Fe-Si-B-P-Cu nanocrystalline alloys with minor Mn addition](#)

AIP Advances **8**, 056110 (2018); 10.1063/1.5007109

[Microstructure, soft magnetic properties and applications of amorphous Fe-Co-Si-B-Mo-P alloy](#)

AIP Advances **8**, 056116 (2018); 10.1063/1.5007781

[Minor-Cu doped soft magnetic Fe-based FeCoBCSiCu amorphous alloys with high saturation magnetization](#)

AIP Advances **8**, 056115 (2018); 10.1063/1.5006404

[New Fe-based soft magnetic alloys composed of ultrafine grain structure](#)

Journal of Applied Physics **64**, 6044 (1988); 10.1063/1.342149

[Fe-Si-B-P-C-Cu nanocrystalline soft magnetic powders with high \$B_s\$ and low core loss](#)

AIP Advances **7**, 056111 (2017); 10.1063/1.4978408

[Soft magnetic characteristics of laminated magnetic block cores assembled with a high \$B_s\$ nanocrystalline alloy](#)

AIP Advances **8**, 056640 (2018); 10.1063/1.5006098



Don't let your writing
keep you from getting
published!

AIP | Author Services

Learn more today!

Effect of magnetic field annealing on soft magnetic properties of $\text{Co}_{71}\text{Fe}_2\text{Si}_{14-x}\text{B}_{9+x}\text{Mn}_4$ amorphous alloys with low permeability

Xingdu Fan,^{1,2} Meng Li,¹ Tao Zhang,^{1,2} Chenchen Yuan,^{1,2}
and Baolong Shen^{1,2,3,a}

¹School of Materials Science and Engineering, Southeast University, Nanjing 211189, PR China

²Jiangsu Key Laboratory for Advanced Metallic Materials, Nanjing 211189, PR China

³Institute of Massive Amorphous Metal Science, China University of Mining and Technology, Xuzhou 221116, PR China

(Presented 10 November 2017; received 29 September 2017; accepted 23 October 2017; published online 11 December 2017)

The effect of transverse magnetic field annealing (TFA) on soft magnetic properties of $\text{Co}_{71}\text{Fe}_2\text{Si}_{14-x}\text{B}_{9+x}\text{Mn}_4$ amorphous alloys was investigated with the aim of reducing effective permeability (μ_e). It was revealed that the increasing B content improved thermal stability, increased saturation magnetic flux density (B_s) of as-quenched alloys, while the samples exhibited a slightly larger coercivity (H_c) when the atom percentages of Si and B were similar. Permeability decreased dramatically after TFA. The decrease of permeability mainly depended on annealing temperature and magnetic field intensity. Besides, flat hysteresis loops were obtained after TFA, Lorentz micrograph observation revealed the TFA sample exhibited denser magnetic domain walls, which confirmed it was more difficult to be saturated. The $\text{Co}_{71}\text{Fe}_2\text{Si}_9\text{B}_{14}\text{Mn}_4$ alloy was successfully prepared with low μ_e of 3020, low H_c of 1.7 A/m and high resistance to DC bias 6 times that of as-quenched alloy at the DC field of 300 A/m. © 2017 Author(s). All article content, except where otherwise noted, is licensed under a Creative Commons Attribution (CC BY) license (<http://creativecommons.org/licenses/by/4.0/>). <https://doi.org/10.1063/1.5006989>

I. INTRODUCTION

Co-based amorphous alloys have been widely applied in power electronic devices due to their high permeability, low core loss and low saturation magnetostriction.¹⁻⁴ However, in some special applications, such as direct current (DC) superposition, or work in a large excitation magnetic field, it is required that the material demonstrates low permeability, because high permeability can easily lead to the saturation of magnetic devices and even loss of efficacy. Generally, there are two ways to improve saturation resistance. The first way is to achieve high saturation magnetic flux density (B_s) that requires high content of ferromagnetic elements. The other is to reduce the permeability which mainly depends on alloy composition and heat treatment condition.

CoFeSiBMn amorphous alloy has been developed with low permeability, low core loss as well as the giant magneto-impedance effect.⁴⁻⁶ However, there are few reports on the preparation technics of this alloy. As is known to all, the metalloid elements such as B, C, Si, P, etc. take efficient effect on amorphous forming ability (AFA) and soft magnetic properties of amorphous alloys, the addition of metalloid elements can effectively improve AFA, but also decrease the B_s .⁷⁻¹⁰ Meanwhile, it has been pointed out that transverse magnetic field annealing (TFA) can further optimize soft magnetic properties because the induced uniaxial anisotropy (K_u) can make magnetic domain rearrange along with the magnetic field direction, flatten the hysteresis loop hence decrease the permeability.^{11,12} Therefore, with the aim of synthesizing Co-based amorphous alloys combined with relatively high

^a Author to whom correspondence should be addressed. Electronic mail: blshen@seu.edu.cn (Baolong Shen)

B_s and low permeability, $\text{Co}_{71}\text{Fe}_2\text{Si}_{14-x}\text{B}_{9+x}\text{Mn}_4$ amorphous alloys were prepared. The influence of Si and B content and TFA on thermal stability, magnetic domain structures and soft magnetic properties were investigated.

II. EXPERIMENTAL

Alloy ingots with nominal compositions of $\text{Co}_{71}\text{Fe}_2\text{Si}_{14-x}\text{B}_{9+x}\text{Mn}_4$ ($x = 0-5$) were made by alloying the mixtures of Co (99.99 mass%), Fe (99.99 mass%), Si (99.99 mass%), B (99.5 mass%) and Mn (99.5 mass%) in an arc furnace under an argon atmosphere. Alloy ribbons were prepared by single copper roller melt-spinning. The width and thickness were 1 mm and 28-32 μm , respectively. Thermal stability was evaluated by differential scanning calorimeter (DSC) under a flowing highly purified argon atmosphere with a heating rate of 0.67 $^\circ\text{C}/\text{s}$. Ribbon samples were annealed under vacuum by magnetic field furnace followed by furnace cooling. The samples were placed in a furnace chamber to ensure magnetic field direction parallel to the width of ribbon. Microstructures were identified by Lorentz-transmission electron microscopy (Lorentz-TEM). B_s was measured by a vibrating sample magnetometer (VSM) under a maximum applied field of 800 kA/m. Coercivity (H_c) was measured by *DC* B-H loop tracer under a maximum applied field of 1 kA/m. Permeability was measured with an impedance analyzer under a field of 1 A/m. Resistance to *DC* bias was identified by an impedance analyzer under applied *DC* field from 100 to 400 A/m.

III. RESULT AND DISCUSSION

According to the XRD results, all alloys exhibit amorphous structure feature, indicating good amorphous forming ability. Figure 1 shows the DSC curves of $\text{Co}_{71}\text{Fe}_2\text{Si}_{14-x}\text{B}_{9+x}\text{Mn}_4$ melt-spun ribbons. It can be seen that there are two sharp exothermic peaks for the alloy with $x = 0$, indicating the crystallization process includes two stages. With increasing B content, the crystallization peaks change gradually from two peaks into one, along with the rising of initial crystallization temperature (T_{x1}) and the first top crystallization peak temperature (T_{p1}), which means more complex phases are formed, the higher the thermal stability is. Then the crystallization peak transforms into two peaks again. Meanwhile, the Curie temperature (T_C) increases obviously, which further confirms the improvement of thermal stability.

Figure 2 shows the dependence of magnetic properties on variation of Si and B content for $\text{Co}_{71}\text{Fe}_2\text{Si}_{14-x}\text{B}_{9+x}\text{Mn}_4$ as-quenched alloys. According to the results, B_s increases gradually with richer B content due to the augmenting relative mass percentage of ferromagnetic elements Fe and Co, as the atomic mass of B is less than Si element, the increasing B content reduces the relative mass

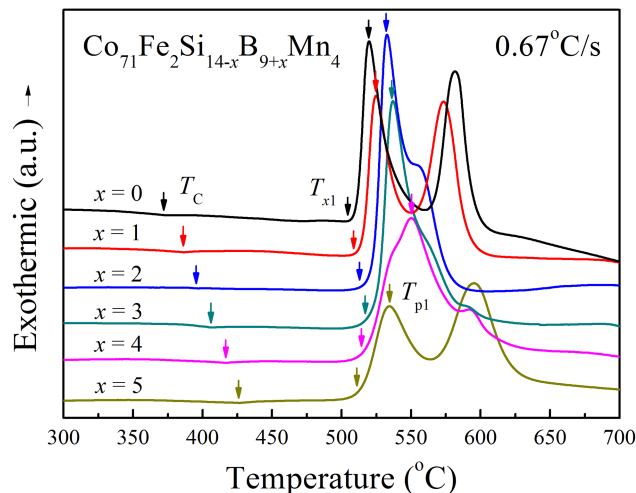


FIG. 1. DSC curves of $\text{Co}_{71}\text{Fe}_2\text{Si}_{14-x}\text{B}_{9+x}\text{Mn}_4$ melt-spun ribbons.

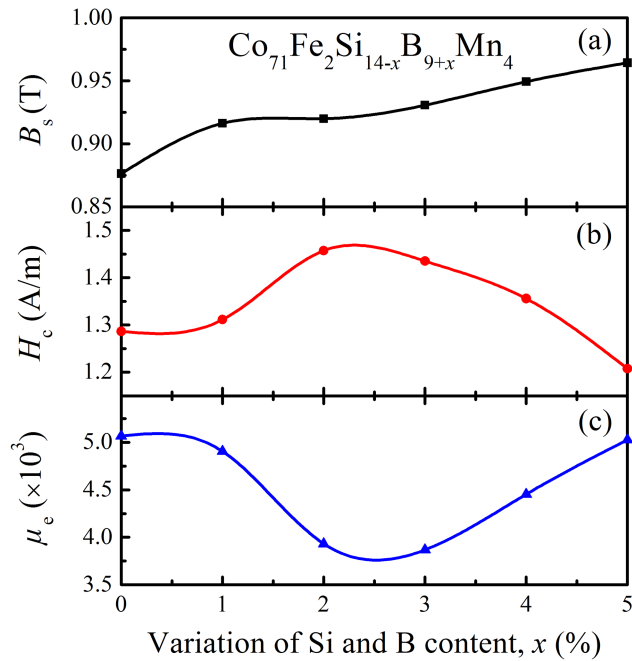


FIG. 2. The dependence of magnetic properties with (a) B_s , (b) H_c and (c) μ_e on variation of Si and B content x .

ratio of the two elements. Besides, it is possible that the increase of B_s relates to the difference in the extra-nuclear structure of Si and B atoms.¹³ There are 4 half-full electrons in the outermost shell for Si atom and it is easy to form sp hybridization, leading to the stable electronic structure. While B has only 3 outermost electrons, the relatively active performance can easily provide empty orbits in the process of electron pair interaction, which is advantageous to the interaction of magnetic moment, leading to the increase in magnetization.

The value of H_c takes no monotonous variation tendency but it still can be seen that the alloys exhibit slightly larger H_c when the atom percentages of Si and B are similar. This phenomenon can be interpreted from the relaxation effects due to local structural rearrangements.^{14,15} The atomic radius of B is far smaller than Co, therefore it is easy to get into atom gaps in the stacking structure of amorphous alloys. As a result, the atoms rearrangement can easily occur, the relaxation susceptibility is decreased which reduces the relaxation H_c . Although the atomic radius of Si and Co is similar, the co-ownership of outer electrons also lead Si atom to enter the gaps hence decreases H_c . But once the Si and B content are close, the influence is restricted, causing the augmentation of relaxation H_c . While the effective permeability (μ_e) takes a contrary variation trend compared to H_c , notes that these alloys possess relatively low μ_e with values of 3870-5060 because of the addition of Mn element, as it is reported that the atomic magnetic moment is arranged in antiparallel for Mn atom due to the negative exchange integration, which greatly deteriorates the permeability.^{13,16}

In order to obtain low permeability, transverse magnetic field annealing was carried out for the alloys. Before TFA, the ribbon samples were first initially stress relief annealed at 415 °C for 5 minutes followed by furnace cooling to the transverse magnetic field annealing temperature (T_{TFA}). Figure 3 (a) shows the dependence of permeability on frequency for $\text{Co}_{71}\text{Fe}_2\text{Si}_9\text{B}_{14}\text{Mn}_4$ amorphous alloy annealed at different T_{TFA} . Here the applied transverse magnetic field intensity (TFI) and annealing time (t_{TFA}) is 550 Oe and 30 minutes, respectively. It is found that permeability decreases dramatically after TFA and trends to a constant at the frequency range from 1k to 1M Hz. The μ_e first decreases and reaches its minimum value of 3460 at 240 °C, then μ_e increases gradually with the rising T_{TFA} . It is noted that there is a sharp decrease for permeability at $T_{\text{TFA}} = 330$ °C, which may be caused by the transition from ferromagnetism to paramagnetism that is induced by magnetic field, as 330 °C is approaching T_C . According to the result, 240 °C is fixed for the T_{TFA} . Figure 3 (b) shows

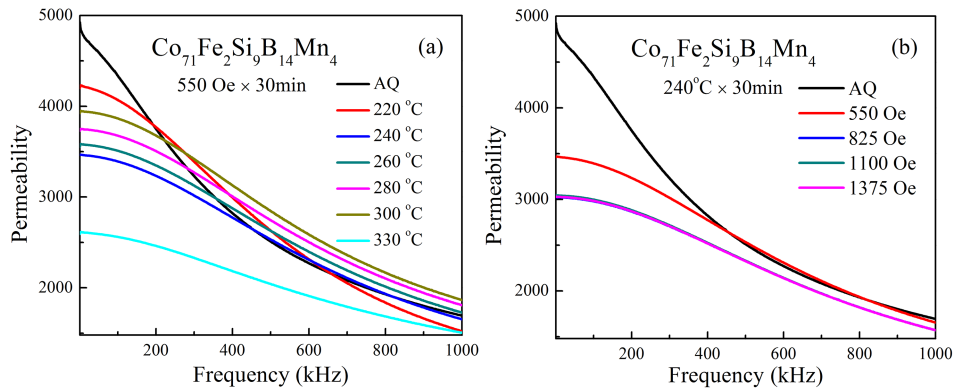


FIG. 3. The dependence of permeability on frequency of $\text{Co}_{71}\text{Fe}_2\text{Si}_9\text{B}_{14}\text{Mn}_4$ amorphous alloy annealed at different (a) transverse magnetic field annealing temperature and (b) transverse magnetic field intensity.

the dependence of permeability on frequency for $\text{Co}_{71}\text{Fe}_2\text{Si}_9\text{B}_{14}\text{Mn}_4$ annealed at different TFI. It can be seen that with strengthening TFI, there is a further decrease of permeability. But when TFI is above 825 Oe, the decreasing trend is not evident as the sample may be saturated and the magnetic domain is possibly oriented consentaneous under the field of 825 Oe.

Figure 4 shows the hysteresis loop of $\text{Co}_{71}\text{Fe}_2\text{Si}_9\text{B}_{14}\text{Mn}_4$ amorphous alloy annealed at different TFI, the inset is a partial enlargement of it. According to the results, flat hysteresis loops are obtained after TFA, which means it is more difficult for the TFA samples to be saturated. Meanwhile, when TFI is above 825 Oe, the slope of the hysteresis loop is even smaller than that of 500 Oe, further confirms the lower permeability. Besides, the alloy exhibits the lowest H_c of 1.7 A/m under TFI of 825 Oe. Therefore, the TFI is fixed as 825 Oe.

Figure 5 shows the magnetic domain walls in $\text{Co}_{71}\text{Fe}_2\text{Si}_9\text{B}_{14}\text{Mn}_4$ ribbon samples imaged by Lorentz-TEM, where magnetic domain walls appear as dark and bright line contrasts. The samples exhibit different domain structures. For as-quenched sample, the domain wall is mainly single-lined and sparse. But the TFA sample exhibits obviously denser magnetic domain walls. The dark-dark and bright-bright lines cross each other, forming domain kinks as indicated by the white bars in figure 5 (b), which act as pinning to the domain wall movement.¹⁷ That is why the TFA sample is more difficult to be saturated. It needs to be pointed out that we also investigated the dependence of permeability on different annealing time, but longer t_{TFA} did not have a significant effect on permeability compared with that of T_{TFA} and TFI. At the same time, longer t_{TFA} also leads to the enlargement of H_c . According to the above results, the permeability is mainly depends on T_{TFA} and TFI.

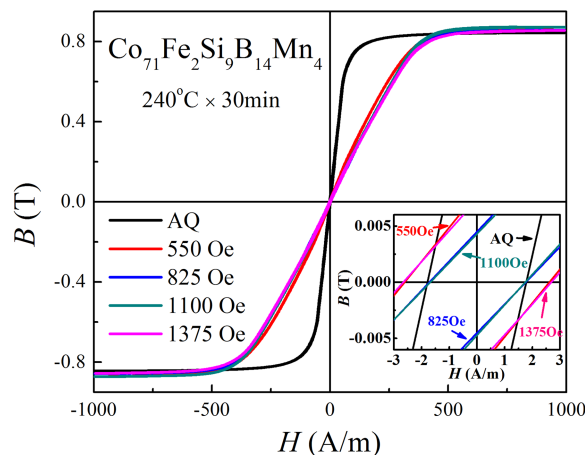


FIG. 4. The hysteresis loop of $\text{Co}_{71}\text{Fe}_2\text{Si}_9\text{B}_{14}\text{Mn}_4$ amorphous alloy annealed at different transverse magnetic field intensity.

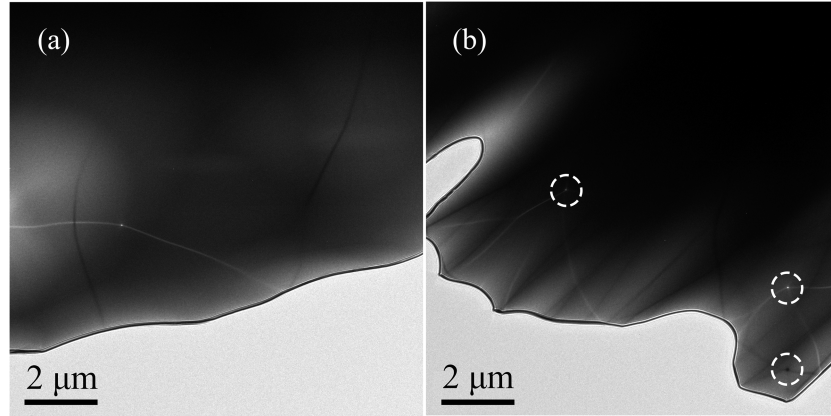


FIG. 5. Lorentz micrograph images of $\text{Co}_{71}\text{Fe}_2\text{Si}_9\text{B}_{14}\text{Mn}_4$ alloy (a) as-quenched and (b) annealed at 240 °C for 30 minutes under transverse magnetic field intensity of 825 Oe.

TABLE I. Soft magnetic properties of $\text{Co}_{71}\text{Fe}_2\text{Si}_{14-x}\text{B}_{9+x}\text{Mn}_4$ amorphous alloys annealed at 240 °C for 30 minutes under TFI of 825 Oe. The symbols μ_{300} and μ_{400} stand for permeability under applied DC field of 300 A/m and 400 A/m, respectively.

Alloy	H_c (A/m)	μ_e (1kHz)	μ_{300} (1kHz)	μ_{400} (1kHz)	μ_{300}/μ_e (%)	μ_{400}/μ_e (%)
$\text{Co}_{71}\text{Fe}_2\text{Si}_{14}\text{B}_9\text{Mn}_4$	1.8	3400	2680	1530	78.8	45.0
$\text{Co}_{71}\text{Fe}_2\text{Si}_{13}\text{B}_{10}\text{Mn}_4$	1.7	3320	2660	1730	80.1	52.1
$\text{Co}_{71}\text{Fe}_2\text{Si}_{12}\text{B}_{11}\text{Mn}_4$	1.6	3520	3100	2180	88.1	61.9
$\text{Co}_{71}\text{Fe}_2\text{Si}_{11}\text{B}_{12}\text{Mn}_4$	1.5	3280	2880	2140	87.8	65.2
$\text{Co}_{71}\text{Fe}_2\text{Si}_{10}\text{B}_{13}\text{Mn}_4$	1.5	3260	2820	2080	86.5	63.8
$\text{Co}_{71}\text{Fe}_2\text{Si}_9\text{B}_{14}\text{Mn}_4$	1.7	3020	2760	2190	91.4	72.5
$\text{Co}_{71}\text{Fe}_2\text{Si}_9\text{B}_{14}\text{Mn}_4\text{-AQ}$	1.2	4930	730	550	14.8	11.2

Table I summarizes the soft magnetic properties of $\text{Co}_{71}\text{Fe}_2\text{Si}_{14-x}\text{B}_{9+x}\text{Mn}_4$ amorphous alloys annealed at 240 °C for 30 minutes under TFI of 825 Oe compared with those of $\text{Co}_{71}\text{Fe}_2\text{Si}_9\text{B}_{14}\text{Mn}_4$ as-quenched alloy. Though H_c is slightly larger than those of as-quenched alloys after TFA, they still exhibit low values of 1.5-1.8 A/m. The TFA alloys exhibit relatively constant permeability at applied DC field of 300 A/m, reflecting high resistance to DC bias. Meanwhile, μ_{300}/μ_e and μ_{400}/μ_e show increasing tendency with increasing B content, which indicates the improvement of resistance to DC bias. As a result, the $\text{Co}_{71}\text{Fe}_2\text{Si}_9\text{B}_{14}\text{Mn}_4$ alloy was successfully prepared with low H_c of 1.7 A/m, low μ_e of 3020 and high resistance to DC bias above 6 times that of as-quenched alloy at the DC field of 300 A/m and 400 A/m. What is more, the B₁₄ alloy also exhibits a higher B_s of 0.96 T. The combination of low μ_e , good soft magnetic properties and high resistance to DC bias promises a potential application in DC superposition area.

IV. CONCLUSION

In conclusion, the effect of transverse magnetic field annealing on soft magnetic properties of $\text{Co}_{71}\text{Fe}_2\text{Si}_{14-x}\text{B}_{9+x}\text{Mn}_4$ amorphous alloys was investigated. The results show that the increasing B content improves the thermal stability and B_s of as-quenched alloys. Transverse magnetic field annealing takes great influence on magnetic domain structures and permeability, the decrease of permeability mainly depends on the annealing temperature and magnetic field intensity. The $\text{Co}_{71}\text{Fe}_2\text{Si}_{14-x}\text{B}_{9+x}\text{Mn}_4$ alloys annealed at 240 °C for 30 minutes under TFI of 825 Oe exhibit low μ_e of 3020-3400, low H_c of 1.5-1.8 A/m and relatively constant permeability at applied DC field. The resistance to DC bias such as μ_{300}/μ_e and μ_{400}/μ_e is 5-6 times that of $\text{Co}_{71}\text{Fe}_2\text{Si}_9\text{B}_{14}\text{Mn}_4$ as-quenched alloy.

ACKNOWLEDGMENTS

This work was supported by the National Natural Science Foundation of China (Grant Nos. 51401052, 51471050 and 51601038), Key Program of National Natural Science Foundation of China (Grant No. 51631003), the National Key Research and Development Program of China (Grant No. 2016YFB0300500) and Jiangsu Key Laboratory for Advanced Metallic Materials (Grant No. BM2007204).

- ¹ METGLAS® Inc, Metglas® 2714A magnetic alloy, <<http://www.metglas.com>>.
- ² M. Yagi, T. Sato, Y. Sakaki, T. Sawa, and K. Inomata, *J. Appl. Phys.* **64**, 6050 (1988).
- ³ VACUUMSCHMELTZ GmbH & Co. KG, Soft magnetic materials and semi-finished products, <<http://www.vacuumschmelze.com>>.
- ⁴ J. Petzold, *J. Magn. Magn. Mater.* **84**, 242 (2002).
- ⁵ K. S. Byon, S. C. Yu, and C. G. Kim, *J. Appl. Phys.* **89**, 11 (2001).
- ⁶ I. Z. Rahman, Md. Kamruzzaman, and M. A. Rahman, *J. Mater. Proc. Tech.* **153**, 791 (2004).
- ⁷ C. D. Graham and T. Egami, *IEEE Trans. Mag.* **15**, 1398 (1979).
- ⁸ B. L. Shen, Y. J. Zhou, C. T. Chang, and A. Inoue, *J. Appl. Phys.* **101**, 09N101 (2007).
- ⁹ T. D. Shen, B. R. Sun, and S. W. Xin, *Intermetallics* **65**, 111 (2015).
- ¹⁰ W. M. Yang, C. Wan, H. S. Liu, Q. Li, Q. Q. Wang, H. Li, J. Zhou, L. Xue, B. L. Shen, and A. Inoue, *Mater. Design* **129**, 63 (2017).
- ¹¹ K. Suzuki and G. Herzer, *Scripta Mater.* **67**, 548 (2012).
- ¹² G. Herzer, *Acta Mater.* **67**, 718 (2013).
- ¹³ S. Chikazumi, *Physics of Ferromagnetism* (Oxford Sci. Pub., 2009).
- ¹⁴ H. Kronmüller, *J. Appl. Phys.* **52**, 1859 (1981).
- ¹⁵ F. E. Luborsky, *Amorphous Metallic Alloys* (Butterworths Pub., 1983).
- ¹⁶ J. M. D. Coey, *Magnetism and Magnetic Materials*, Cambridge Univ. Pub. (2009).
- ¹⁷ Z. Akase, S. Aizawa, D. Shindo, P. Sharma, and A. Makino, *J. Magn. Magn. Mater.* **375**, 10 (2015).